THE JOURNAL OF PHYSICAL CHEMISTRY C

Article

pubs.acs.org/JPCC

CdSe/CdSe$_{1-x}$Te$_x$ Core/Crown Heteronanoplatelets: Tuning the Excitonic Properties without Changing the Thickness

Yusuf Kelestemur,[†] Burak Guzelturk,[†] Onur Erdem,[†] Murat Olutas,[†,‡] Talha Erdem,[†] Can Firat Usanmaz,[†] Kivanc Gungor,[†] and Hilmi Volkan Demir*[,†,§]

[†]Department of Electrical and Electronics Engineering, Department of Physics, UNAM—Institute of Materials Science and Nanotechnology, Bilkent University, Ankara 06800, Turkey

[‡]Department of Physics, Abant Izzet Baysal University, Bolu 14280, Turkey

[§]Luminous! Center of Excellence for Semiconductor Lighting and Displays, School of Electrical and Electronic Engineering, School of Physical and Materials Sciences, School of Materials Science and Nanotechnology, Nanyang Technological University, Singapore 639798, Singapore

Supporting Information

ABSTRACT: Here we designed and synthesized CdSe/CdSe$_{1-x}$Te$_x$ core/crown nanoplatelets (NPLs) with controlled crown compositions by using the core-seeded-growth approach. We confirmed the uniform growth of the crown regions with well-defined shape and compositions by employing transmission electron microscopy, X-ray photoelectron spectroscopy, and X-ray diffraction. By precisely tuning the composition of the CdSe$_{1-x}$Te$_x$ crown region from pure CdTe (x = 1.00) to almost pure CdSe doped with several Te atoms (x = 0.02), we achieved tunable excitonic properties without changing the thickness of the NPLs and demonstrated the evolution of type-II electronic structure. Upon increasing the Te concentration in the crown region, we obtained continuously tunable photoluminescence peaks within the range of ∼570 nm (for CdSe$_{1-x}$Te$_x$ crown with x = 0.02) and ∼660 nm (for CdSe$_{1-x}$Te$_x$ crown with x = 1.00). Furthermore, with the formation of the CdSe$_{1-x}$Te$_x$ crown region, we observed substantially improved photoluminescence quantum yields (up to ∼95%) owing to the suppression of nonradiative hole trap sites. Also, we found significantly increased fluorescence lifetimes from ∼49 up to ∼326 ns with increasing Te content in the crown, suggesting the transition from quasi-type-II to type-II electronic structure. With their tunable excitonic properties, this novel material presented here will find ubiquitous use in various efficient light-emitting and -harvesting applications.

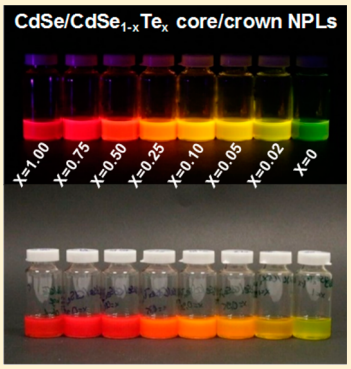

INTRODUCTION

Free-standing semiconductor nanoplatelets (NPLs) with magic-sized vertical thickness, also widely known as colloidal quantum wells, have recently emerged as a highly promising class of semiconductor nanocrystals.[1−3] Owing to tight quantum confinement only in the vertical direction, the NPLs exhibit unique thickness-dependent optical properties, including narrower emission bandwidth,[4] giant oscillator strength together with ultrafast radiative fluorescence lifetimes,[2,4] and extremely large linear[5,6] and nonlinear absorption cross sections.[7] In addition to the core-only NPLs having different vertical thicknesses and chemical compositions,[8−11] different heteroarchitectures of NPLs, such as core/crown (laterally grown shell),[12,13] core/shell (vertically grown shell),[14,15] and core/crown/shell[16] NPLs, can be synthesized to further engineer their electronic structure and optical properties. Also, depending on the band alignment between the core and crown or shell materials, either type-I- or type-II-like electronic structures can be achieved,[17−19] which results in favorable properties for various optoelectronic applications.

To date, core/crown and core/shell NPLs with type-I electronic structure, in which electron and hole wave functions are confined in the same region of the NPLs, have been synthesized and studied extensively. In the core/crown and core/shell architectures, the passivation of the periphery (sidewalls) and larger surfaces of core-only NPLs has been shown to improve the photoluminescence quantum yield (PLQY) and stability.[12,20] Also, by growing CdS crown and shell regions, increased absorption cross section and suppressed Auger recombination with reduced blinking have been demonstrated.[21,22] Moreover, tunable emission behavior has been realized with the synthesis of inverted CdS/CdSe core/crown heterostructure.[23] All of these appealing properties have led to the demonstrations of low threshold lasing[22,24−26] and light-emitting diodes (LEDs) with high color purity[27] by using core/crown and core/shell NPLs having type-I-like electronic structure. On the other hand, NPLs having type-II-like

Received: November 23, 2016
Revised: January 31, 2017
Published: February 1, 2017

DOI: 10.1021/acs.jpcc.6b11809
J. Phys. Chem. C 2017, 121, 4650−4658

electronic structure have not been studied extensively, despite their significant potential for optical gain and light-harvesting applications.

Recently, several groups, including ours, have reported the synthesis and characterization of CdSe/CdTe core/crown NPLs having type-II electronic structure with their exciting excitonic properties.[28−31] In these NPLs, electrons are localized in the CdSe core while holes are confined in the CdTe crown, forming spatially indirect excitons. Therefore, they exhibit strongly red-shifted emission together with significantly increased radiative florescence lifetimes. Also, these NPLs feature remarkably high PLQY (up to ∼50%) when compared to other classes of semiconductor nanocrystals having type-II electronic structure.[28,29] In addition, it has been shown that owing to their large in-plane exciton mobility, ultrafast time scale charge separation at the core/crown interface enables the suppression of nonradiative recombination.[31] However, due to the quantum confinement occurring only in the vertical direction, CdSe/CdTe core/crown NPLs suffer from the limited tunability of their optical properties. Although the emission of CdSe/CdTe core/crown NPLs can be tuned within the range of ∼620−660 nm during the growth of the CdTe crown region, it quickly saturates at ∼660 nm and suffers from the lower PLQY. Therefore, to further engineer their excitonic properties for advanced optoelectronic applications, novel NPL architectures are desired.

To address this need, here we synthesized CdSe/$CdSe_{1-x}Te_x$ NPLs with precisely tuned crown composition ranging from pure CdTe (x = 1.00) to almost pure CdSe doped with several Te atoms (x = 0.02) for tuning their excitonic properties. With the synthesis of core/crown NPLs having the same vertical thickness together with the same quantum confinement, we showed the systematic evolution of type-II electronic structure experimentally. Also, by using the transmission electron microscopy, X-ray photoelectron spectroscopy, and X-ray diffraction, we demonstrated the highly monodisperse and uniform growth of $CdSe_{1-x}Te_x$ crown regions with targeted chemical compositions. In addition, we observed that the increase in the Te concentration within the crown region shifts the emission peak wavelength of CdSe/$CdSe_{1-x}Te_x$ NPLs continuously to lower energies with increased radiative fluorescence lifetimes. This behavior is explained by the transition from initial quasi-type-II electronic structure, where holes are localized around Te atoms and electrons spread over both the core and crown region, to type-II electronic structure, where holes are confined to the crown region and electrons are localized in the core region.[32] Moreover, CdSe/$CdSe_{1-x}Te_x$ core/crown NPLs exhibit substantially improved PLQY (up to 95%), which can be attributed to the ultrafast localization of the photogenerated holes around Te atoms and their radiative recombination on the time scale of several tens of nanoseconds instead of nonradiative hole trapping commonly observed in NPLs.[31,33] With their engineered and promising excitonic properties, CdSe/$CdSe_{1-x}Te_x$ core/crown NPLs are highly promising for high-efficiency light-emitting and -harvesting applications.

EXPERIMENTAL SECTION

Chemicals. Cadmium nitrate tetrahydrate [$Cd(NO_3)_2 \cdot 4H_2O$] (99.997% trace metals basis), sodium myristate (>99%), technical-grade 1-octadecene (ODE), selenium (Se) (99.99% trace metals basis), tellurium (Te) (99.99% trace metals basis), cadmium acetate dihydrate [$Cd(OAc)_2 \cdot 2H_2O$] (>98%), technical-grade trioctylphosphine (TOP) (90%), and technical-grade oleic acid (OA) (90%) were purchased from Sigma-Aldrich. Hexane, ethanol, and methanol were purchased from Merck Millipore and used without any further purification.

Preparation of Cadmium Myristate. Cadmium myristate was synthesized by following the protocol reported in the literature.[12] For a typical synthesis, 1.23 g of cadmium nitrate tetrahydrate was mixed with 40 mL of methanol, and 3.13 g of sodium myristate was mixed with 250 mL of methanol. When the cadmium nitrate tetrahydrate and sodium myristate powders were completely dissolved, the solutions were mixed and stirred vigorously for ∼1 h. Subsequently, the white cadmium myristate powders were precipitated by using a centrifuge and dissolved in methanol. The cleaning step with methanol was repeated at least three times to remove any unreacted and/or excess precursors. Finally, the precipitated powders of cadmium myristate were kept overnight under vacuum for complete drying.

Synthesis of the 4-ML-Thick CdSe NPLs. CdSe core NPLs having four monolayer (4 ML) thickness with an additional layer of Cd atoms were synthesized by using the slightly modified recipe from the literature.[12] For a typical synthesis, 340 mg of cadmium myristate, 24 mg of Se, and 30 mL of ODE were put into a three-neck flask, and the solution was evacuated at 100 °C for 1 h. After the complete removal of oxygen, water, and any other volatile solvents, the temperature of the solution was set to 240 °C under an argon atmosphere. When the color of the solution turned to bright yellowish, 110−120 mg of cadmium acetate dihydrate was injected into the reaction solution. Subsequently, the solution was kept for 10 min at 240 °C for further growth of NPLs. Then, with the injection of 1 mL of OA, the synthesis was stopped and the temperature of the solution was decreased to room temperature. As-synthesized NPLs were precipitated by adding ethanol. Finally, the precipitated NPLs were dissolved in hexane and stored for further crown coating steps.

Preparation of Anisotropic Growth Mixture for $CdSe_{1-x}Te_x$ Crown Region. Anisotropic growth mixture was prepared by using the previously published procedure with slight modifications.[12] For the cadmium precursor, 480 mg of cadmium acetate dihydrate, 340 μL of OA, and 2 mL of ODE were put into a three-neck flask. Then, the temperature of the solution was raised to 100 °C under ambient atmosphere and regular sonication. The heating and sonication processes continued alternatingly until the formation of a homogeneous gel having whitish color. Following that, the cadmium precursor was stored for the successive crown coating. For the Se and Te precursors, 1 M TOP−Se and TOP−Te solutions were prepared inside a glovebox. Then, these solutions were diluted with the addition of ODE to achieve 0.03 M ODE−TOP−Te injection solution for the CdTe crown growth. Depending on the desired composition of the crown region, the concentration of injection solution was adjusted by mixing the 1 M TOP−Se and 1 M TOP−Te solutions.

Synthesis of 4-ML-Thick CdSe/$CdSe_{1-x}Te_x$ Core/Crown NPLs. By using our previously published procedure, we executed the uniform growth of the $CdSe_{1-x}Te_x$ crown region around CdSe core NPLs.[29] For a typical CdTe crown coating, 1 mL of 4-ML-thick CdSe NPLs dissolved in hexane (0.1 mL of stock solution dissolved in 3 mL of hexane has an optical density of ∼0.6 at 350 nm), 5 mL of ODE, 400 μL of cadmium precursor, and 50 μL of OA were put into a 50 mL three-neck

DOI: 10.1021/acs.jpcc.6b11809
J. Phys. Chem. C 2017, 121, 4650−4658

flask. Then, the solution was evacuated at 100 °C for 1 h. After the complete removal of water, hexane, and any other organic solvents, the temperature of the solution was set to 240 °C under argon flow for the growth of the CdTe crown region. When the temperature reaches 240 °C, a certain amount of ODE−TOP−Te (0.03 M) solution was injected at a rate of 8 mL/h. To control the size of the crown region, the injection amount can be varied between 0.40 and 1.50 mL. After the complete injection of Te precursor, the resulting mixture was further annealed for 5 min at 240 °C. Then, the reaction was stopped and cooled down to room temperature. Owing to their increased lateral size, as-synthesized CdSe/CdTe core/crown NPLs were precipitated by centrifugation without adding any solvents, and they were dissolved in hexane for further characterization steps. For the synthesis of $CdSe_{1-x}Te_x$ crown region having different compositions, the same protocol described for the growth of pure CdTe crown was used. The composition of the crown region can be tuned by simply changing the ratio of Te and Se in the injection precursor.

Preparation of NPL Integrated Light-Emitting Diode (LED). A LED of the NPLs was prepared by embedding them into a two-component silicone (Dow Corning, OE-6630). For this purpose, the solvent from 750 μL of $CdSe/CdSe_{1-x}Te_x$ core/crown NPLs (~7.2 mg) was evaporated, and the NPLs were dispersed in 50 μL of hexane followed by the addition of 250 μL of the silicone mixture. To remove the air bubbles and remaining solvent, the mixture was kept under vacuum for 30 min. Subsequently, ca. 200 μL of the NPL−silicone mixture was placed on a glass substrate and hardened at 75 °C overnight. Finally, the obtained film was transferred onto an Edison near-UV-LED emitting at 400 nm. The optical characterizations of the LED were carried out by measuring the emission intensity using an Ocean Optics integrating sphere and Maya 2000 spectrometer. CIE 1931 color coordinates were calculated using an in-house written MATLAB code.

Photoluminescence Quantum Yield Measurements. The PLQY measurements were carried out using the methodology reported by de Mello et al.[34] The measurement setup was constructed using a HoribaYvon integrating sphere and Maya 2000 spectrometer.

RESULTS AND DISCUSSION

In this study, we synthesized $CdSe/CdSe_{1-x}Te_x$ core/crown NPLs having different crown compositions by employing the core-seeded-growth approach. First, we started with the synthesis of 4-ML-thick CdSe core-only NPLs having an additional layer of Cd atoms owing to their well-defined synthesis conditions (see the Experimental Section for details). Absorption and photoluminescence (PL) spectra of CdSe core NPLs are given in Figure 1a. Thanks to the synthesis of CdSe core NPLs having magic size vertical thickness and atomically flat surfaces, they exhibit a very narrow emission bandwidth (~9 nm) with moderately high PLQY (30−40%). From the absorption spectra, splitting of sharp excitonic features, including electron-light hole (~480 nm) and electron-heavy hole transitions (~512 nm), is observed, suggesting the formation of a quantum-well-like electronic structure.[2] Also, the highly monodisperse and uniform growth of 4-ML-thick CdSe core-only NPLs can be clearly seen in the high-angle annular dark-field scanning transmission electron microscopy (HAADF-STEM) images given in Figure 1b. They feature almost rectangular shape with lateral dimensions of 16.44 ± 1.72 and 12.60 ± 1.47 nm. These CdSe core-only NPLs were

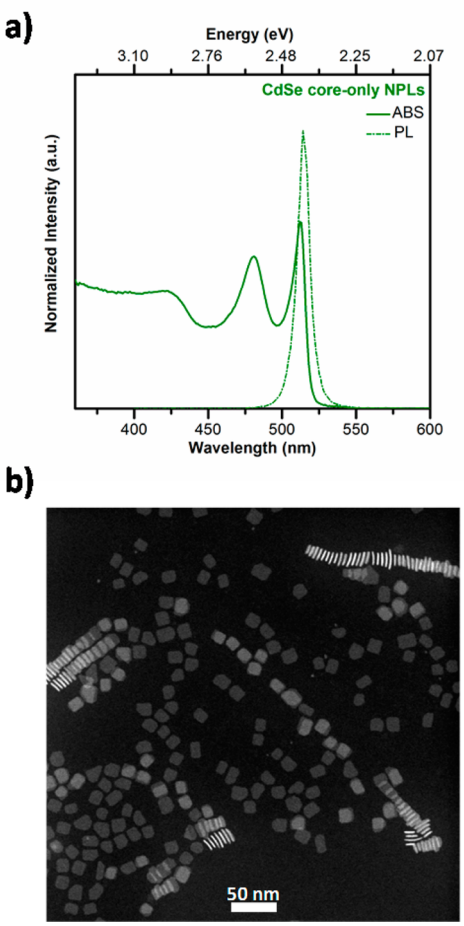

Figure 1. (a) Absorption (solid line) and photoluminescence (dotted−dashed line) spectra and (b) high-angle annular dark-field scanning transmission electron microscopy (HAADF-STEM) images of the 4-ML-thick CdSe core-only NPLs dissolved in hexane at room temperature, having a lateral size of 16.4 ± 1.7 nm by 12.6 ± 1.5 nm.

used as a seed for the further synthesis of $CdSe/CdSe_{1-x}Te_x$ core/crown NPLs with varied crown compositions.

By using freshly synthesized CdSe core-only NPLs as a seed, we grew $CdSe_{1-x}Te_x$ crown region with different crown compositions. First, we determined the optimal crown size by synthesizing core/crown NPLs having pure CdTe crown regions with different lateral sizes. While CdSe/CdTe core/crown NPLs having a smaller CdTe crown exhibit additional lateral confinement,[28,29,35] CdSe/CdTe core/crown NPLs with a larger CdTe crown suffer from serious stability issues and lower PLQY (see the Supporting Information). Therefore, we preferred the synthesis of core/crown NPLs with medium crown size exhibiting pure vertical confinement together with improved PLQY and stability. For the synthesis of $CdSe/CdSe_{1-x}Te_x$ core/crown NPLs having a similar crown size to that of the optimized pure CdTe crown region, the same amount of anisotropic growth mixture precursors was injected. In addition, by changing the concentration of Te and Se in the injection solution, the composition of the crown region was tuned and $CdSe/CdSe_{1-x}Te_x$ core/crown NPLs with a specific crown composition ranging from pure CdTe crown to almost pure CdSe crown doped with several Te atoms were synthesized (see Experimental Section for details).

We carried out the structural characterizations of $CdSe/CdSe_{1-x}Te_x$ core/crown NPLs, including transmission electron

DOI: 10.1021/acs.jpcc.6b11809
J. Phys. Chem. C 2017, 121, 4650−4658

microscopy, X-ray photoelectron spectroscopy, and X-ray diffraction, for a better understanding of the size, shape, and composition of the crown region. HAADF-TEM images of CdSe/CdSe$_{1-x}$Te$_x$ core/crown NPLs having different crown compositions are shown in Figure 2. As can be clearly seen

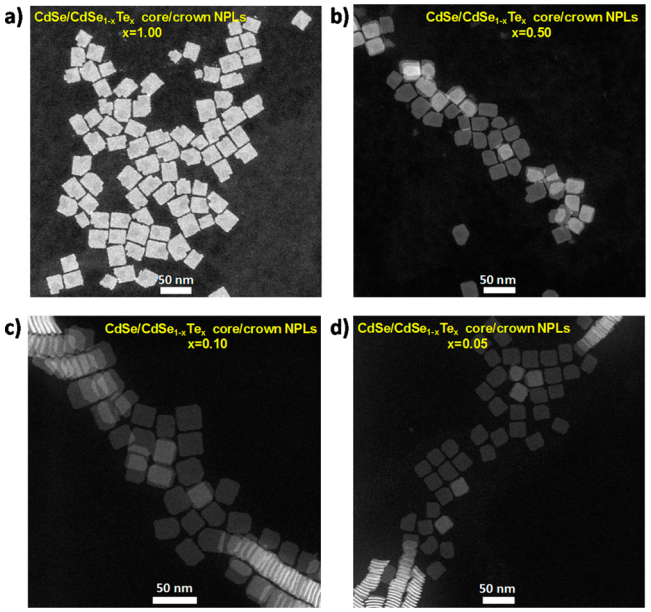

Figure 2. High-angle annular dark-field scanning transmission electron microscopy (HAADF-STEM) images of the CdSe/CdSe$_{1-x}$Te$_x$ core/crown NPLs for different Te compositions (a) x = 1.00, (b) x = 0.50, (c) x = 0.10, and (d) x = 0.05 in the crown region.

from the HAADF images, the resulting core/crown NPLs having different crown compositions exhibit high monodispersity in size and uniform growth of the crown region in the lateral direction with sharp boundaries. Owing to the same amount of anisotropic growth mixture injection for the formation of crown regions, the lateral areas of the crown with different crown compositions were found to be similar (Table S1, Supporting Information). Furthermore, with increasing Se composition in the crown region, the shape of the core/crown NPLs was changed from rectangular to almost square shape, which can be attributed to the variation of the favorable growth direction depending on the composition. For example, while CdSe/CdTe core/crown NPLs (x = 1.00) feature lateral dimensions of 29.11 ± 3.00 and 22.79 ± 2.20 nm, CdSe/CdSe$_{1-x}$Te$_x$ core/crown NPLs (x = 0.02) have lateral dimensions of 25.69 ± 1.61 and 22.97 ± 1.98 nm. In addition, we performed energy-dispersive X-ray spectroscopy (EDX) for single CdSe/CdSe$_{1-x}$Te$_x$ core/crown NPLs (x = 1.00, 0.50, and 0.25) to investigate the uniformity of core/crown architecture and chemical compositions (Figure S4, Supporting Information). The results showed that while the CdSe core region generally located in the inner part of the NPLs, it was covered with a laterally extended CdSe$_{1-x}$Te$_x$ crown region. Also, it has been observed that the composition of the CdSe$_{1-x}$Te$_x$ region is almost similar to the concentration of the injection solutions, suggesting that the composition of the crown region can be precisely tuned.

We also analyzed the composition of the CdSe$_{1-x}$Te$_x$ crown region by using X-ray photoelectron spectroscopy (XPS). With the contribution from both the core and crown regions, the concentration of Se was found to be higher than that of Te in the ensemble measurements (except x = 1.00 and 0.75). Then, by using the ratio of lateral size between the core and crown obtained from the HAADF-TEM images, the composition of the crown regions was calculated from the ensemble measurements (Table 1 and the Supporting Information). The

Table 1. Chemical Composition of CdSe$_{1-x}$Te$_x$ Crown Region Obtained by XPS and XRD

chemical composition (x) of the CdSe$_{1-x}$Te$_x$ crown region		
injected	XPS	XRD
1.00	1.00	1.00
0.75	0.64	0.76
0.50	0.46	0.58
0.25	0.22	0.17
0.10	0.10	0.14
0.05	0.07	0.08
0.02	0.06	0.03

compositions of the crown regions were found to be similar to the concentration of the injection solutions, except the CdSe/CdSe$_{1-x}$Te$_x$ core/crown NPLs (x = 0.02) having very low Te concentration in the crown region. This can be attributed to the very weak intensity levels collected from the sample, resulting in an overestimated calculation (Figure S5, Supporting Information). Thus, the synthesis of CdSe/CdSe$_{1-x}$Te$_x$ core/crown NPLs having similar crown areas with desired composition strongly suggest the similar reactivities of Te and Se, enabling the achievement of tunable excitonic properties in a controlled way.

We also studied the crystal structure of CdSe/CdSe$_{1-x}$Te$_x$ core/crown NPLs having different crown compositions with powder X-ray diffraction. The powder diffraction patterns of CdSe/CdSe$_{1-x}$Te$_x$ core/crown NPLs are presented in Figure 3.

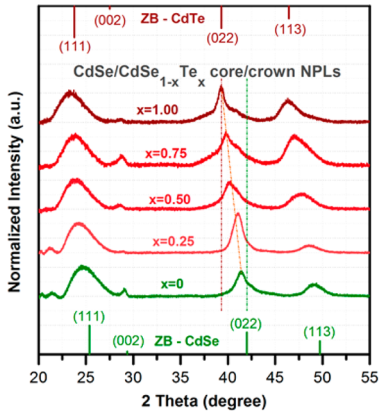

Figure 3. X-ray diffraction (XRD) patterns of the 4-ML-thick CdSe core-only NPLs and the CdSe/CdSe$_{1-x}$Te$_x$ core/crown NPLs having different crown compositions. The green (on the bottom) and the brown bars (on the top) show the diffraction peaks of the bulk CdSe and bulk CdTe having zinc blende (ZB) structure, respectively.

CdSe core-only NPLs exhibit zinc blende crystal structure with broader diffraction peaks owing to their finite crystal size. Furthermore, the relative intensities of diffraction peaks were observed to be different when compared to those of their bulk counterparts, suggesting the growth of an anisotropic shape with a preferred growth direction. In addition, as the crown regions having different compositions were grown, the initial

DOI: 10.1021/acs.jpcc.6b11809
J. Phys. Chem. C 2017, 121, 4650−4658

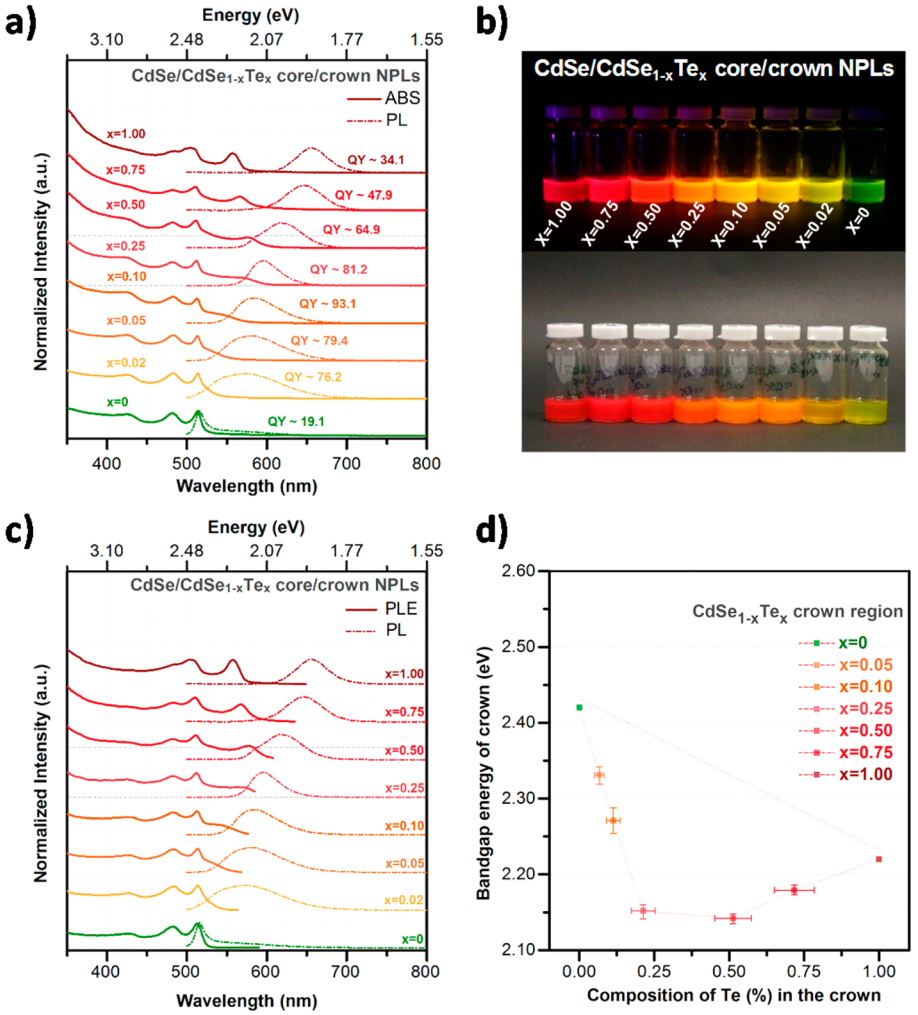

Figure 4. (a) Evolution of the absorption and photoluminescence spectra along with PLQY as a function of the $CdSe_{1-x}Te_x$ crown region composition. (b) The real color images of $CdSe/CdSe_{1-x}Te_x$ core/crown NPLs having different crown compositions dissolved in hexane under UV light (top) and ambient light (bottom). (c) Photoluminescence excitation (PLE) spectra of the $CdSe/CdSe_{1-x}Te_x$ core/crown NPLs together with their photoluminescence and (d) extracted band gap energy of the crown region as a function of the composition of the Te in the crown.

zinc blende crystal structure was preserved. However, increasing the concentration of Te in the crown region continuously shifts the diffraction peaks to lower angles, which further suggests the formation of an alloyed crown region. Moreover, by applying Vegard's law for the (022) plane, we roughly estimated the composition of the crown region, which is tabulated in Table 1. However, due to contribution from both the CdSe core and $CdSe_{1-x}Te_x$ crown regions in the diffraction patterns with their broader diffraction peaks, the compositions estimated from the powder diffraction patterns exhibit slight deviations.

After the complete analysis of the structural characterization, including the size, shape, and composition of the crown region, we systematically studied the resulting optical properties of $CdSe/CdSe_{1-x}Te_x$ core/crown NPLs. Their absorption and PL spectra are presented in Figure 4a. With the formation of a pure CdTe crown region, a new peak emerges around ~556 nm and makes a strong contribution to the absorption of the core/crown NPLs in the lower-energy side of the spectrum. Since the crown region was grown only in the lateral dimensions, the excitonic features of CdSe core NPLs remained almost in the same spectral positions. However, owing to formation and recombination of spatially indirect excitons at the core/crown interface, where electrons are localized in the CdSe core region and holes are confined to the CdTe crown region, they exhibit significantly red-shifted emission (~656 nm) with a broadened spectrum. In addition, when compared to other classes of semiconductor nanocrystals having type-II electronic structure and CdSe core-only NPLs, they exhibit relatively high PLQY (~30−50%). However, owing to the pure vertical confinement in this material system, their emission wavelengths remain almost in the same spectral position upon changing the size of the CdTe crown region and suffer from the limited tunability.

To realize tunable excitonic properties without changing the vertical thickness of the NPLs, we engineered the band gap of the crown region by adjusting the composition. As can be seen from Figure 4a, increasing the concentration of Se in the crown region allowed for continuously tuning the emission of core/crown NPLs from ~660 nm (for $CdSe_{1-x}Te_x$ crown with x = 1.00) to ~570 nm (for $CdSe_{1-x}Te_x$ crown with x = 0.02). The continuous shift of the emission spectrum can be explained by the decrease in the hole energy levels by tailoring the composition of the crown region, which can be clearly seen from the extracted relative band offsets of the $CdSe/CdSe_{1-x}Te_x$ core/crown NPLs having different compositions (Figure 5a,b).[32] Thus, the recombination energy of the

DOI: 10.1021/acs.jpcc.6b11809
J. Phys. Chem. C 2017, 121, 4650−4658

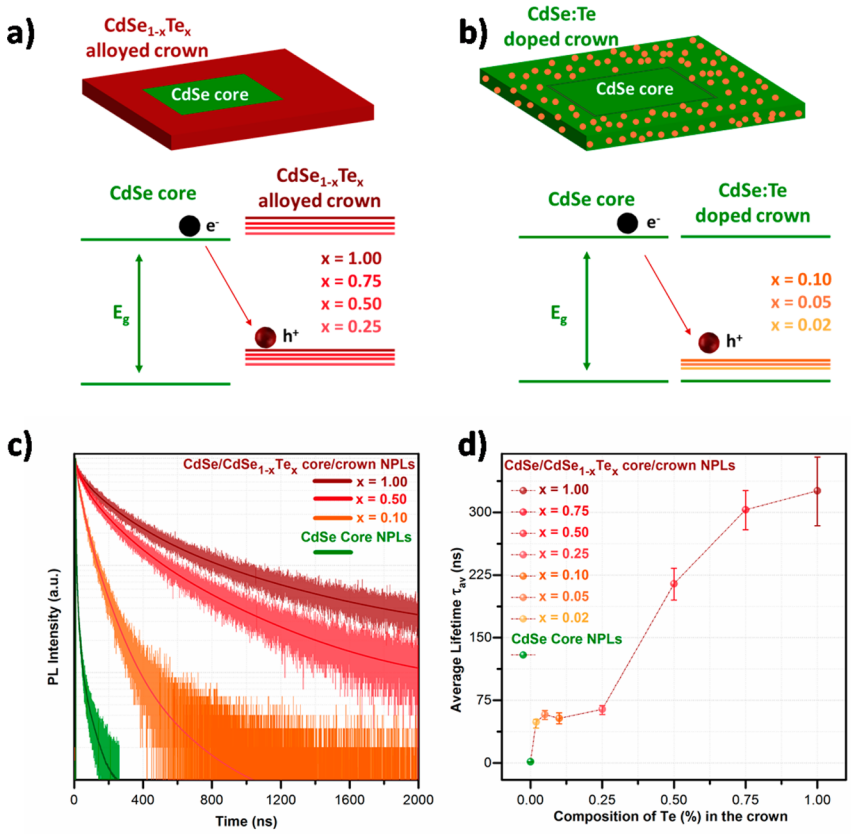

Figure 5. Schematic demonstration of band diagrams of the CdSe/CdSe$_{1-x}$Te$_x$ core/crown NPLs for $x \geq 0.25$ (a) and for $x \leq 0.10$ (b). (c) Time-resolved fluorescence decay curves of the CdSe core and CdSe/CdSe$_{1-x}$Te$_x$ core/crown NPLs for different crown region compositions (e.g., x = 1.00, 0.50, and 0.10). The solid lines on the decay curves represent the four-exponential fitting curves. (d) Amplitude-averaged fluorescence lifetimes of the CdSe/CdSe$_{1-x}$Te$_x$ core/crown NPLs with tuned crown compositions.

electrons localized in the CdSe core region and the holes confined in the CdSe$_{1-x}$Te$_x$ crown region increases and results in a continuous blue-shifting in the emission spectrum. Also, CdSe/CdSe$_{1-x}$Te$_x$ core/crown NPL exhibit significantly broadened emission spectrum as compared to the CdSe core-only NPLs (~40 meV). This is a common feature of colloidal semiconductor nanocrystals having type-II-like electronic structure and can be explained by the spatially indirect exciton recombination.[19,28] In addition, the same excitonic features observed from the PLE spectra of CdSe/CdSe$_{1-x}$Te$_x$ core/crown NPLs taken at different emission wavelengths have ruled out the possibility of inhomogeneous broadening due to the composition variation in the crown region and suggested the formation of a crown region with well-defined and homogeneous compositions (Figure S7, Supporting Information).

It is also important to note that while CdSe/CdSe$_{1-x}$Te$_x$ core/crown NPLs ($x \geq 0.25$) feature broadened emission spectra (~140−190 meV) with respect to CdSe core-only NPLs, CdSe/CdSe$_{1-x}$Te$_x$ core/crown NPLs ($x \leq 0.10$) exhibit further broadened emission (up to ~360 meV) with increasing Se concentration in the crown region. This behavior can be explained by the transition from type-II electronic structure (for $x \geq 0.25$), where spatially indirect excitons recombine at the core/crown interface, to quasi-type-II electronic structure (for $x \leq 0.10$), where Te atoms act as deep hole-trap sites. In previous studies, similar behavior was also observed for Te-doped CdSe quantum dots and attributed to the size distribution of quantum dots, resulting in different quantum confinement among the quantum dots within the ensemble solution.[36,37] However, because of the pure vertical quantum confinement in our NPLs, the further broadened emission behavior cannot be explained by the difference in the quantum confinement. Therefore, together with the homogeneous broadening, the fluctuation of the Te composition and variation of Te location within the NPLs should be responsible for the further broadening.

We also measured the PLQY of CdSe/CdSe$_{1-x}$Te$_x$ core/crown NPLs. With the laterally extended CdSe$_{1-x}$Te$_x$ crown region, CdSe/CdSe$_{1-x}$Te$_x$ core/crown NPLs exhibit substantially improved PLQY (up to ~95%) as compared to that having a pure CdTe or CdSe crown region. The relatively high PLQY of CdSe/CdSe$_{1-x}$Te$_x$ core/crown NPLs with respect to other classes of semiconductor nanocrystals having type-II electronic structure can be explained by several factors. First, with increasing Se concentration in the crown region, the overlap of electron and hole wave functions in the CdSe/CdSe$_{1-x}$Te$_x$ core/crown NPLs is significantly increased when compared to CdSe/CdSe$_{1-x}$Te$_x$ core/crown NPLs having a pure CdTe crown region (x = 1.00), resulting in the enhanced PLQY. Second, the substitution of Te atoms with Se atoms in the crown region decreases the lattice mismatch between the core and crown region. Thus, the possibility of strain and/or defect formation, which act as trap sites, is reduced. Finally, the localization of the photogenerated holes in the CdSe$_{1-x}$Te$_x$ crown region and/or around Te atoms, which is followed by radiative recombination, competed with the nonradiative hole trapping commonly observed in NPLs owing to absence of proper surface passivation. In other words, the localization of

DOI: 10.1021/acs.jpcc.6b11809
J. Phys. Chem. C 2017, 121, 4650−4658

the holes in the engineered $CdSe_{1-x}Te_x$ crown and/or around Te atoms, instead of being captured by surface trap sites, and their radiative recombination on the time scale of several tens of nanoseconds contributed to the improved the PLQY.[38] Also, the observation of both the ultrafast exciton localization (~0.65 ps) at the core/crown interface in CdSe/CdTe core/crown NPLs and ultrafast hole trapping around Te atoms on a subpicosecond time scale in Te-doped CdSe quantum dots further supports this hypothesis.[31,39] The dramatically improved PLQY of CdSe core NPLs from ~19.1% to 76.2% upon replacing several Se atoms by Te atoms in the CdSe crown region (x = 0.02) shows the efficient localization of photogenerated holes around Te atoms instead of their capture by the surface trap sites.

In addition to the tunable emission behavior of CdSe/$CdSe_{1-x}Te_x$ core/crown NPLs with significantly improved PLQY, these NPLs show interesting absorption behavior. Owing to the growth of the crown regions only in the lateral direction, excitonic absorption features of CdSe core NPLs preserved their spectral positions for all different crown compositions. On the other hand, the excitonic absorption features of the $CdSe_{1-x}Te_x$ crown region exhibit a nonlinear relationship between the compositions (Figure 4d). From the absorption spectra of the core/crown NPLs, we extracted the band gap energies of the crown regions having different compositions (see the Supporting Information). It is observed that the band gap energies of the crown region do not change linearly with the composition as predicted by Vegard's law and exhibit a strongly nonlinear effect, which is called as "optical bowing". This kind of behavior has already been observed for alloyed nanocrystal quantum dots and attributed to structural and electronic factors, including different atomic radii and the electronegativity of the ions.[40]

For a deeper understanding of the excitonic properties of CdSe/$CdSe_{1-x}Te_x$ core/crown NPLs depending on the composition of the crown region, we performed time-resolved fluorescence spectroscopy (TRF). TRF measurements were carried out under low excitation intensities to avoid multi-exciton generation by using core/crown NPL solutions having low concentrations. Fluorescence decay curves of CdSe core and CdSe/$CdSe_{1-x}Te_x$ core/crown NPLs (for x = 1.00, 0.50, and 0.10) and their amplitude-averaged fluorescence lifetimes (τ_{av}) are presented in Figure 5c,d. Owing to the complex emission kinetics of NPLs, the decay curves were fitted by using four-exponential decay functions so that the reduced χ^2 values remain about 1 with uniform residuals. As can be seen from Figure 5b, with increasing Te concentration in the crown region, we observed continuously increased τ_{av} from ~1.5 ns (for CdSe core only NPLs) to ~326.2 ns (for CdSe/$CdSe_{1-x}Te_x$ core/crown NPLs with x = 1.00). Also, while CdSe/$CdSe_{1-x}Te_x$ core/crown NPLs (x = 0.02) had a τ_{av} of ~49.2 ns, CdSe/$CdSe_{1-x}Te_x$ core/crown NPLs (x = 1.00) having a pure CdTe crown region exhibit a strongly elongated τ_{av} of ~326.2 ns. This can be explained by transitioning from a quasi-type-II electronic structure to a type-II electronic structure. With the substitution of several Se atoms with Te in the crown region, CdSe/$CdSe_{1-x}Te_x$ core/crown NPLs ($x \leq$ 0.10) possess quasi-type-II structure, where Te atoms acts as deep hole trap sites and holes are localized around Te atoms (Figure 5b). Our findings are also strongly consistent with the recent study of Tenne et al., who reported that the fluorescence lifetime of Te-doped CdSe NPLs was dominated by the lifetime component of ~50 ns.[41] On the other hand, CdSe/$CdSe_{1-x}Te_x$ core/crown NPLs having a higher Te concentration ($x \geq$ 0.25) exhibit type-II electronic structure, where holes are localized around the crown region and electrons are confined to the core. This increased separation of electron and hole wave functions results in increased fluorescence lifetimes in CdSe/$CdSe_{1-x}Te_x$ core/crown NPLs. Therefore, this series of observations demonstrate the evolution of the band alignment from quasi-type-II to type-II experimentally.

Finally, we demonstrated a proof-of-concept color-converting LED employing CdSe/$CdSe_{1-x}Te_x$ core/crown NPLs. For this purpose, we prepared a film of NPLs (x = 0.05) in a commercially available silicone and integrated it onto a near-UV-LED emitting at 400 nm. The spectrum of the obtained LED is presented in Figure 6, along with the chromaticity

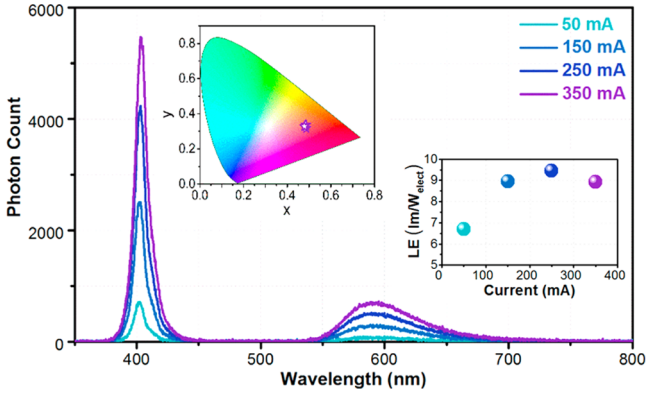

Figure 6. Emission spectra of the NPL-integrated LED at varying currents along with luminous efficiency (LE) (inset, right) and CIE 1931 color coordinates (inset, left).

coordinates and luminous efficiency (LE) in the insets. We observe that the emitted yellowish color corresponds to around (0.48, 0.33) on the CIE 1931 chromaticity diagram and its LE takes values up to 9.5 lm/W_{elect}.

In conclusion, we have demonstrated the synthesis of CdSe/$CdSe_{1-x}Te_x$ core/crown NPLs with precisely tuned crown composition from pure CdTe to almost pure CdSe doped with several Te atoms. Thanks to the same vertical quantum confinement in the core/crown architectures, we have shown experimentally the evolution of type-II electronic structure. Also, with engineering the band gap of the crown region, we have successfully tuned the excitonic properties of the NPLs without changing their thickness. Moreover, by the substitution of several Se atoms with Te in the crown region, we have substantially improved the PLQY (up to 95%), which can be attributed to the suppressed nonradiative hole trap sites. When compared to previously synthesized doped semiconductor nanocrystals having lower PLQY, the near unity PLQY of CdSe/$CdSe_{1-x}Te_x$ core/crown NPLs can be attributed to the large in-plane exciton mobility and higher exciton binding energies observed in these atomically flat semiconductor NPLs. Considering these appealing and tunable excitonic properties, CdSe/$CdSe_{1-x}Te_x$ core/crown NPLs have become highly attractive for advanced optoelectronic applications. With their large Stoke-shifted emission and near unity PLQY, CdSe/$CdSe_{1-x}Te_x$ core/crown NPLs have become highly promising candidates for highly efficient luminescent solar concentrators and low threshold optical gain.

DOI: 10.1021/acs.jpcc.6b11809
J. Phys. Chem. C 2017, 121, 4650−4658

■ ASSOCIATED CONTENT

Supporting Information

The Supporting Information is available free of charge on the ACS Publications website at DOI: 10.1021/acs.jpcc.6b11809.

Absorption and photoluminescence spectra of the CdSe/CdTe core/crown NPLs having different CdTe crown size; high-angle annular dark-field scanning transmission electron microscopy (HAADF-STEM) images of the CdSe/$CdSe_{1-x}Te_x$ core/crown NPLs; quantitative line EDX analysis from single CdSe/$CdSe_{1-x}Te_x$ core/crown NPLs; X-ray photoelectron spectra of CdSe/$CdSe_{1-x}Te_x$ core/crown NPLs; calculation of the composition of $CdSe_{1-x}Te_x$ crown region from XPS; X-ray diffraction patterns of CdSe/$CdSe_{1-x}Te_x$ core/crown NPLs; photoluminescence excitation (PLE) spectra of CdSe/$CdSe_{1-x}Te_x$ core/crown NPLs; time-resolved fluorescence (TRF) spectroscopy measurements of CdSe/$CdSe_{1-x}Te_x$ core/crown NPLs; determination of the band gap energy of the $CdSe_{1-x}Te_x$ crown region (PDF)

■ AUTHOR INFORMATION

Corresponding Author

*E-mail: volkan@bilkent.edu.tr or hvdemir@ntu.edu.sg.

ORCID

Burak Guzelturk: 0000-0003-1977-6485

Hilmi Volkan Demir: 0000-0003-1793-112X

Notes

The authors declare no competing financial interest.

■ ACKNOWLEDGMENTS

The authors gratefully acknowledge the financial support from Singapore National Research Foundation under the programs of NRF-NRFI2016-08 and NRF-CRP-6-2010-02 and the Science and Engineering Research Council, Agency for Science, Technology and Research (A*STAR) of Singapore; EU-FP7 Nanophotonics4Energy NoE; and TUBITAK EEEAG 114E449 and 114F326. H.V.D. acknowledges support from ESF-EURYI and TUBAGEBIP. Y.K., O.E., and T.E. acknowledge support from TUBITAK BIDEB.

■ REFERENCES

(1) Ithurria, S.; Dubertret, B. Quasi 2D Colloidal CdSe Platelets with Thicknesses Controlled at the Atomic Level. *J. Am. Chem. Soc.* **2008**, *130*, 16504−16505.

(2) Ithurria, S.; Tessier, M. D.; Mahler, B.; Lobo, R. P. S. M.; Dubertret, B.; Efros, A. L. Colloidal Nanoplatelets with Two-Dimensional Electronic Structure. *Nat. Mater.* **2011**, *10*, 936−941.

(3) Lhuillier, E.; Pedetti, S.; Ithurria, S.; Nadal, B.; Heuclin, H.; Dubertret, B. Two-Dimensional Colloidal Metal Chalcogenides Semiconductors: Synthesis, Spectroscopy, and Applications. *Acc. Chem. Res.* **2015**, *48*, 22−30.

(4) Tessier, M. D.; Javaux, C.; Maksimovic, I.; Loriette, V.; Dubertret, B. Spectroscopy of Single CdSe Nanoplatelets. *ACS Nano* **2012**, *6*, 6751−6758.

(5) Achtstein, A. W.; Antanovich, A.; Prudnikau, A.; Scott, R.; Woggon, U.; Artemyev, M. Linear Absorption in CdSe Nanoplates: Thickness and Lateral Size Dependency of the Intrinsic Absorption. *J. Phys. Chem. C* **2015**, *119*, 20156−20161.

(6) Yeltik, A.; Delikanli, S.; Olutas, M.; Kelestemur, Y.; Guzelturk, B.; Demir, H. V. Experimental Determination of the Absorption Cross-Section and Molar Extinction Coefficient of Colloidal CdSe Nanoplatelets. *J. Phys. Chem. C* **2015**, *119*, 26768−26775.

(7) Olutas, M.; Guzelturk, B.; Kelestemur, Y.; Yeltik, A.; Delikanli, S.; Demir, H. V. Lateral Size-Dependent Spontaneous and Stimulated Emission Properties in Colloidal CdSe Nanoplatelets. *ACS Nano* **2015**, *9*, 5041−5050.

(8) Pedetti, S.; Nadal, B.; Lhuillier, E.; Mahler, B.; Bouet, C.; Abécassis, B.; Xu, X.; Dubertret, B. Optimized Synthesis of CdTe Nanoplatelets and Photoresponse of CdTe Nanoplatelets Films. *Chem. Mater.* **2013**, *25*, 2455−2462.

(9) Li, Z.; Qin, H.; Guzun, D.; Benamara, M.; Salamo, G.; Peng, X. Uniform Thickness and Colloidal-Stable CdS Quantum Disks with Tunable Thickness: Synthesis and Properties. *Nano Res.* **2012**, *5*, 337−351.

(10) Bhandari, G. B.; Subedi, K.; He, Y.; Jiang, Z.; Leopold, M.; Reilly, N.; Lu, H. P.; Zayak, A. T.; Sun, L. Thickness-Controlled Synthesis of Colloidal PbS Nanosheets and Their Thickness-Dependent Energy Gaps. *Chem. Mater.* **2014**, *26*, 5433−5436.

(11) Fan, F.; Kanjanaboos, P.; Saravanapavanantham, M.; Beauregard, E.; Ingram, G.; Yassitepe, E.; Adachi, M. M.; Voznyy, O.; Johnston, A. K.; Walters, G.; et al. Colloidal CdSe 1− X S X Nanoplatelets with Narrow and Continuously-Tunable Electroluminescence. *Nano Lett.* **2015**, *15*, 4611−4615.

(12) Tessier, M. D.; Spinicelli, P.; Dupont, D.; Patriarche, G.; Ithurria, S.; Dubertret, B. Efficient Exciton Concentrators Built from Colloidal Core/Crown CdSe/CdS Semiconductor Nanoplatelets. *Nano Lett.* **2014**, *14*, 207−213.

(13) Prudnikau, A.; Chuvilin, A.; Artemyev, M. CdSe−CdS Nanoheteroplatelets with Efficient Photoexcitation of Central CdSe Region through Epitaxially Grown CdS Wings. *J. Am. Chem. Soc.* **2013**, *135*, 14476−14479.

(14) Mahler, B.; Nadal, B.; Bouet, C.; Patriarche, G.; Dubertret, B. Core/Shell Colloidal Semiconductor Nanoplatelets. *J. Am. Chem. Soc.* **2012**, *134*, 18591−18598.

(15) Ithurria, S.; Talapin, D. V. Colloidal Atomic Layer Deposition (c-ALD) Using Self-Limiting Reactions at Nanocrystal Surface Coupled to Phase Transfer between Polar and Nonpolar Media. *J. Am. Chem. Soc.* **2012**, *134*, 18585−18590.

(16) Kelestemur, Y.; Guzelturk, B.; Erdem, O.; Olutas, M.; Gungor, K.; Demir, H. V. Platelet-in-Box Colloidal Quantum Wells: CdSe/CdS@CdS Core/Crown@Shell Heteronanoplatelets. *Adv. Funct. Mater.* **2016**, *26*, 3570−3579.

(17) Hines, M. A.; Guyot-Sionnest, P. Synthesis and Characterization of Strongly Luminescing ZnS-Capped CdSe Nanocrystals. *J. Phys. Chem.* **1996**, *100*, 468−471.

(18) Peng, X.; Schlamp, M. C.; Kadavanich, A. V.; Alivisatos, A. P. Epitaxial Growth of Highly Luminescent CdSe/CdS Core/Shell Nanocrystals with Photostability and Electronic Accessibility. *J. Am. Chem. Soc.* **1997**, *119*, 7019−7029.

(19) Kim, S.; Fisher, B.; Eisler, H.-J.; Bawendi, M. Type-II Quantum Dots: CdTe/CdSe(Core/Shell) and CdSe/ZnTe(Core/Shell) Heterostructures. *J. Am. Chem. Soc.* **2003**, *125*, 11466−11467.

(20) Tessier, M. D.; Mahler, B.; Nadal, B.; Heuclin, H.; Pedetti, S.; Dubertret, B. Spectroscopy of Colloidal Semiconductor Core/Shell Nanoplatelets with High Quantum Yield. *Nano Lett.* **2013**, *13*, 3321−3328.

(21) Kunneman, L. T.; Tessier, M. D.; Heuclin, H.; Dubertret, B.; Aulin, Y. V.; Grozema, F. C.; Schins, J. M.; Siebbeles, L. D. A. Bimolecular Auger Recombination of Electron-Hole Pairs in Two-Dimensional CdSe and CdSe/CdZnS Core/shell Nanoplatelets. *J. Phys. Chem. Lett.* **2013**, *4*, 3574−3578.

(22) She, C.; Fedin, I.; Dolzhnikov, D. S.; Dahlberg, P. D.; Engel, G. S.; Schaller, R. D.; Talapin, D. V. Red, Yellow, Green, and Blue Amplified Spontaneous Emission and Lasing Using Colloidal CdSe Nanoplatelets. *ACS Nano* **2015**, *9*, 9475−9485.

(23) Delikanli, S.; Guzelturk, B.; Hernández-Martínez, P. L.; Erdem, T.; Kelestemur, Y.; Olutas, M.; Akgul, M. Z.; Demir, H. V. Continuously Tunable Emission in Inverted Type-I CdS/CdSe Core/Crown Semiconductor Nanoplatelets. *Adv. Funct. Mater.* **2015**, *25*, 4282−4289.

(24) Guzelturk, B.; Kelestemur, Y.; Olutas, M.; Delikanli, S.; Demir, H. V. Amplified Spontaneous Emission and Lasing in Colloidal Nanoplatelets. *ACS Nano* **2014**, *8*, 6599−6605.
(25) She, C.; Fedin, I.; Dolzhnikov, D. S.; Demortière, A.; Schaller, R. D.; Pelton, M.; Talapin, D. V. Low-Threshold Stimulated Emission Using Colloidal Quantum Wells. *Nano Lett.* **2014**, *14*, 2772−2777.
(26) Grim, J. Q.; Christodoulou, S.; Di Stasio, F.; Krahne, R.; Cingolani, R.; Manna, L.; Moreels, I. Continuous-Wave Biexciton Lasing at Room Temperature Using Solution-Processed Quantum Wells. *Nat. Nanotechnol.* **2014**, *9*, 891−895.
(27) Chen, Z.; Nadal, B.; Mahler, B.; Aubin, H.; Dubertret, B. Quasi-2D Colloidal Semiconductor Nanoplatelets for Narrow Electroluminescence. *Adv. Funct. Mater.* **2014**, *24*, 295−302.
(28) Pedetti, S.; Ithurria, S.; Heuclin, H.; Patriarche, G.; Dubertret, B. Type-II CdSe/CdTe Core/Crown Semiconductor Nanoplatelets. *J. Am. Chem. Soc.* **2014**, *136*, 16430−16438.
(29) Kelestemur, Y.; Olutas, M.; Delikanli, S.; Guzelturk, B.; Akgul, M. Z.; Demir, H. V. Type-II Colloidal Quantum Wells: CdSe/CdTe Core/Crown Heteronanoplatelets. *J. Phys. Chem. C* **2015**, *119*, 2177−2185.
(30) Antanovich, A. V.; Prudnikau, A. V.; Melnikau, D.; Rakovich, Y. P.; Chuvilin, A.; Woggon, U.; Achtstein, A. W.; Artemyev, M. V. Colloidal Synthesis and Optical Properties of Type-II CdSe−CdTe and Inverted CdTe−CdSe Core−wing Heteronanoplatelets. *Nanoscale* **2015**, *7*, 8084−8092.
(31) Wu, K.; Li, Q.; Jia, Y.; McBride, J. R.; Xie, Z.-X.; Lian, T. Efficient and Ultrafast Formation of Long-Lived Charge-Transfer Exciton State in Atomically Thin Cadmium Selenide/Cadmium Telluride Type-II Heteronanosheets. *ACS Nano* **2015**, *9*, 961−968.
(32) Zhang, L.; Lin, Z.; Luo, J.-W.; Franceschetti, A. The Birth of a Type-II Nanostructure: Carrier Localization and Optical Properties of Isoelectronically Doped CdSe:Te Nanocrystals. *ACS Nano* **2012**, *6*, 8325−8334.
(33) Kunneman, L. T.; Schins, J. M.; Pedetti, S.; Heuclin, H.; Grozema, F. C.; Houtepen, A. J.; Dubertret, B.; Siebbeles, L. D. a. Nature and Decay Pathways of Photoexcited States in CdSe and CdSe/CdS Nanoplatelets. *Nano Lett.* **2014**, *14*, 7039−7045.
(34) de Mello, J. C.; Wittmann, H. F.; Friend, R. H. An Improved Experimental Determination of External Photoluminescence Quantum Efficiency. *Adv. Mater.* **1997**, *9*, 230−232.
(35) Ithurria, S.; Bousquet, G.; Dubertret, B. Continuous Transition from 3D to 1D Confinement Observed during the Formation of CdSe Nanoplatelets. *J. Am. Chem. Soc.* **2011**, *133*, 3070−3077.
(36) Avidan, A.; Oron, D. Large Blue Shift of the Biexciton State in Tellurium Doped CdSe Colloidal Quantum Dots. *Nano Lett.* **2008**, *8*, 2384−2387.
(37) Franzl, T.; Müller, J.; Klar, T. A.; Rogach, A. L.; Feldmann, J.; Talapin, D. V.; Weller, H. CdSe:Te Nanocrystals: Band-Edge versus Te-Related Emission. *J. Phys. Chem. C* **2007**, *111*, 2974−2979.
(38) Califano, M.; Gómez-Campos, F. M. Universal Trapping Mechanism in Semiconductor Nanocrystals. *Nano Lett.* **2013**, *13*, 2047−2052.
(39) Avidan, A.; Pinkas, I.; Oron, D. How Quickly Does a Hole Relax into an Engineered Defect State in CdSe Quantum Dots. *ACS Nano* **2012**, *6*, 3063−3069.
(40) Bailey, R. E.; Nie, S. Alloyed Semiconductor Quantum Dots: Tuning the Optical Properties without Changing the Particle Size. *J. Am. Chem. Soc.* **2003**, *125*, 7100−7106.
(41) Tenne, R.; Pedetti, S.; Kazes, M.; Ithurria, S.; Houben, L.; Nadal, B.; Oron, D.; Dubertret, B. From Dilute Isovalent Substitution to Alloying in CdSeTe Nanoplatelets. *Phys. Chem. Chem. Phys.* **2016**, *18*, 15295−15303.

DOI: 10.1021/acs.jpcc.6b11809
J. Phys. Chem. C 2017, 121, 4650−4658